

## SIGMA PHASE PRECIPITATION IN AUSTENITIC STAINLESS STEELS

**Amna Hodžić, Almajda Gigović-Gekić, Raza Sunulahpašić**  
**University of Zenica, Faculty of Metallurgy and Technology**  
**Zenica**  
**Bosnia and Herzegovina**

**Keywords:** austenitic stainless steel,  $\delta$  ferrite,  $\sigma$  phase, precipitation characteristics, mechanical properties, corrosion properties

### ABSTRACT

*The precipitation of sigma ( $\sigma$ ) phase in austenitic stainless steels is a significant subject of many investigations. Exposure of these steels to elevated temperatures (from 600 °C to 900 °C) results in precipitation of  $\sigma$  phase (transformation product from delta ( $\delta$ ) ferrite) which is one of the main reasons for the deterioration austenitic stainless steels properties. It is therefore of considerable interest to study the conditions for  $\sigma$  phase formation, as well as the mechanism of the transformation. This review paper presents overview of precipitation characteristics (including morphologies and precipitation sites) as well as effect of  $\sigma$  phase on properties of austenitic stainless steels. It is particularly highlighted that the precipitation of hard, brittle and nonmagnetic  $\sigma$  phase occurring preferentially at  $\delta/\gamma$  phase boundary and within  $\delta$  ferrite islands (high Cr concentrated region) cause worse mechanical properties (impact toughness and elongation) and corrosion resistance.*

### 1. INTRODUCTION

Austenitic stainless steels (ASS) are the most commonly used stainless steels accounting for more than 70% of the stainless steel world production. Owing to the good combination of mechanical properties (especially strength and toughness) and corrosion resistance, these steels have wide industrial application [1, 2].

This favourable combination of properties is result monophasic ie. austenitic microstructure which stability is accomplished by solution annealing treatment (heating between 1000 °C to 1120 °C and water quenched). However, by changing the chemical composition, especially by increasing the content of alphasene elements (Cr, Si, Ti, Mo, etc.) precipitation of  $\delta$  ferrite in the austenitic matrix can occur.

Exposure of this steel to elevated temperatures results in precipitation of the intermetallic phases (mainly TCP<sup>1</sup> phases:  $\sigma$  (sigma), Laves( $\eta$ ) and chi ( $\chi$ )) and carbides ( $M_{23}C_6$  and MC type) from the austenite and/or  $\delta$  ferrite. However,  $\sigma$  phase formation which is often observed in various series of stainless steel (such as austenitic, ferritic and duplex, in a general manner), commonly in a temperature range from 600°C to 900°C is one of the main reasons for the deterioration austenitic stainless steel properties (mechanical properties, corrosion resistance and weldability), [3, 4, 5, 6].

---

<sup>1</sup>TCP (Topologically Close Packed)

The  $\sigma$  phase can be precipitated under an elevated temperature environment, for example, casting, rolling, welding, forging and heat treatment (annealing or aging).

As a result of the heat treatment temperature,  $\delta$  ferrite can transform in the austenite ( $\gamma$ ) and the  $\sigma$  phase.  $\sigma$  phase occurs in most of the commercial steels, in the temperature interval of 590 °C to 870 °C, but the phase decomposes at temperatures above 1050 °C [3, 6].

Alloying elements modify the conditions of the  $\sigma$  phase formation by their influence on the precipitation kinetics or phase equilibrium.

In the Cr-Ni austenitic steels,  $\sigma$  phase formation is encouraged by increasing Cr content (25wt.%~30wt.%), and is discouraged by an increase in Ni content.

Generally, all ferrite stabilizing elements (chromium(Cr), niobium (Nb), titanium (Ti), tungsten (W)) accelerate the formation of the  $\sigma$  phase, where molybdenum (Mo) and silicon (Si) also extend the stability range of the  $\sigma$  phase at elevated temperatures when they are dissolved in it. Conversely, carbon and nitrogen as the austenite stabilizing elements form compounds which denude the matrix of chromium and therefore retard  $\sigma$  phase formation.

Hence,  $\delta$  ferrite such as Cr rich region (faster diffusion of Cr and other alphasene elements) is a beneficial site for the precipitation of the  $\sigma$  phase whereat the precipitation rate of the  $\sigma$  phase from  $\delta$  ferrite is about 100 times higher than the rate of the  $\sigma$  phase precipitation directly from austenite, [6, 7, 8]. Since the  $\sigma$  phase presence is closely related to the  $M_{23}C_6$  type of carbides there is a preposition that  $M_{23}C_6$  acts as the precursor to the  $\sigma$  phase. Preexistence of carbides in the steel can be an intensifying factor for  $\sigma$  phase formation, as the formed carbides have high chromium content and can act as the source of chromium, [9].

The  $\sigma$  phase is probably the most studied and undesirable intermetallic phase of previously mentioned phases that can occur in ASS. In 1907, even before the discovery of the stainlesssteels, Treitschke and Tamman found that in the binary Fe-Cr system, there was a intermetallic compound of 30wt.% Cr to 50wt.% Cr range. However, its real discovery came only 20 years later when Bain and Griffiths observed in the Fe-Cr-Ni ternary system hard and very brittle phase that they called „B constituent” where „B” stands for brittle.

In 1936, Jett and Foote called it “ $\sigma$  phase” , while in 1951, Bergmann and Shoemaker studied it in details in the Fe–Cr system and identified the crystallographic structure of the  $\sigma$  phase as topologically close packed structure.

In 1966, the  $\sigma$  phase was observed by Hattersley and Hume-Rothery as well as Hall and Algie in austenitic stainless steels, and in the same year  $\sigma$  phase had been found in several binary, ternary and quaternary systems such as Fe-Cr, Fe-Mo, Fe-V, Fe-Mn, Fe-Cr-Ni, Fe-Cr-Mo, Fe-Cr-Mn and Fe-Cr-Ni-Mo, [6, 10].

In the first section of a review paper, the precipitation characteristics (including precipitation sites and morphologies) of  $\sigma$  phase are described, while in the second section, the influence of the  $\sigma$  phase on the properties of austenitic stainless steels is emphasised.

## 2. PRECIPITATION CHARACTERISTIC OF THE SIGMA PHASE

The  $\sigma$  phase is a nonmagnetic intermetallic compound with a tetragonal unit cell containing 32 atoms located in five nonequivalent groups of sites or sublattices (Figure 1) which is characteristic of a topologically close packed structure (TCP phase).

The chemical composition of this phase varies considerably and it is therefore difficult to define this phase in the form of unique formulas (Table 1)

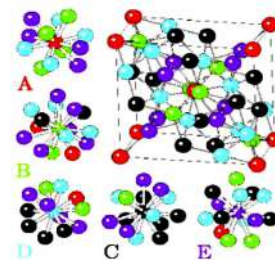


Figure 1. The unit cell of  $\sigma$  phase, and five sublattices A, B, C, D and E with their nearest neighbour shell atoms [12].

[11, 12].

Table 1. Chemical composition and lattice constant of the  $\sigma$  phase [6].

Alloy	Lattice parameters, nm	Composition of phase, wt. %					Formula
		Fe	Cr	Ni	Mo	Si	
Fe-Cr	$a_0 = 0.8799, c_0 = 0.4544$						Fe-Cr
Fe-Mo	$a_0 = 0.9188, c_0 = 0.4812$						Fe-Mo
17Cr-11Ni-2Mo-0.4Ti	—		30	4.3	9	0.8	$(\text{FeNi})_x(\text{CrMo})_y$
17Cr-11Ni-0.9Mo-0.5Ti	—		33	4.5	5.4	0.7	
316	$a_0 = 0.828 \sim 0.838$ $c_0 = 0.4597 \sim 0.4599$	55	29	5	11	—	
316L	$a_0 = 0.921, c_0 = 0.478$						
20Cr-25-34Ni-6.5-8Mo	$a_0 = 0.887, c_0 = 0.461$	35/37	17/26	15/21	21/28	—	
25Cr-20Ni	—	40	46	9.4	—	3	

The  $\sigma$  phase issues from the phase transformation of  $\delta \rightarrow \sigma$  ( $\delta$  ferrite to  $\sigma$  phase), where it precipitates in the high Cr concentrated region of  $\delta$  ferrite and is formed directly from  $\delta$  ferrite particles.

Figures 2a-d show the Time-Temperature-Transformation (TTT) curve of the  $\sigma$  phase of some austenitic stainless steel grades. It can be seen that the nose of the TTT curve is located at a temperature range of 800 °C ~ 850 °C, which means that this temperature range has the fastest precipitation rate.

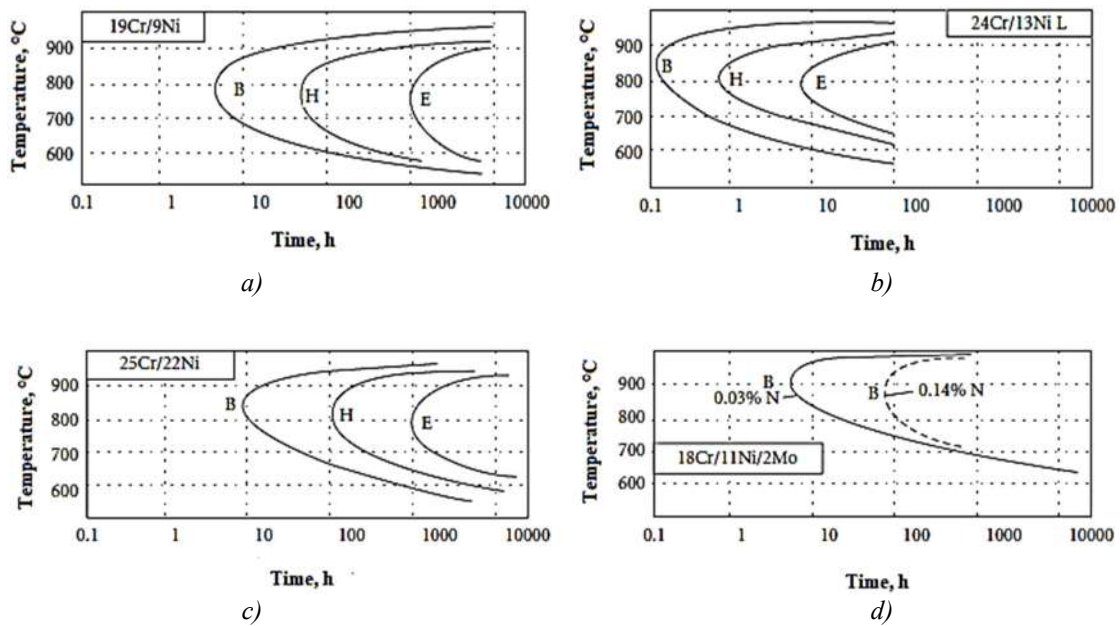


Figure 2. TTT curves of the  $\sigma$  phase in austenitic stainless steels (B: initial precipitation, H: intermediate stage, E: final precipitation stage [6]).

In comparison to steel type 19Cr/9Ni (AISI 304), Figure 2a, with a purely austenitic structure produced by solution annealing,  $\sigma$  phase precipitates at 0.1 h in steel type 24Cr/13Ni L (AISI 309 S) which has a higher precipitation rate than because of its higher chromium content, lower carbon content and the presence of about 15%  $\delta$  ferrite in the structure (Figure 2b). In the case of steel 25Cr/22Ni (AISI 310), Figure 2c, because of increased carbon (0.11%) and nickel contents as well as fully austenitic structure,  $\sigma$  phase precipitation is slowed down to such an extent that it is shifted to considerably longer times. Figure 2d shows the effect of

adding 0.14% nitrogen on the onset of precipitation of the  $\sigma$  phase in low carbon austenitic Cr-Ni-Mo steel (AISI 316). The effect of nitrogen is similar to that of carbon where at the precipitation of all phases not capable to dissolving nitrogen is shifted by nitrogen towards longer times, [6, 13].

## 2.1. Morphology of the sigma phase

The morphologies of  $\sigma$  phase can be classified into dendritic and globular structures. Figures 3a-d show the morphologies of the  $\sigma$  phase in different types of austenitic stainless steel.

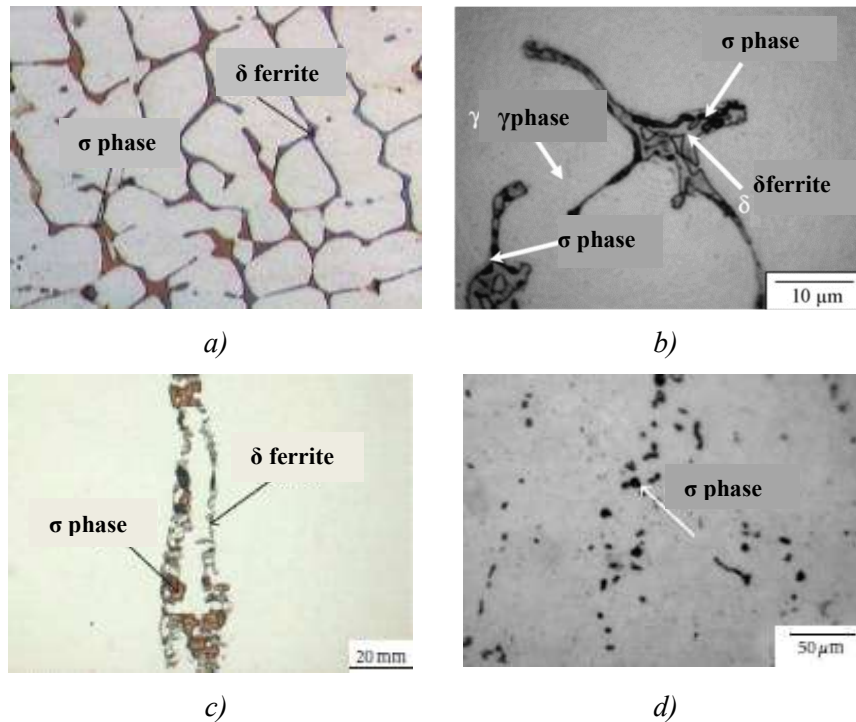


Figure 3. Microstructural observation of the  $\sigma$  phase with different working conditions in austenitic stainless steels: a) as casting AISI 309 LSi stainless steel, b) AISI 304N stainless steel, c) as rolled AISI 316 stainless steel, d) with 50% rolling ratio in AISI stainless steel [6, 14].

The  $\sigma$  phase morphology can be affected by the degree of deformation. In AISI 309 LSi stainless steel (as-casting microstructure)  $\sigma$  phase precipitates in dendrite  $\delta$  ferrite and this is the typical precipitation morphology of the  $\sigma$  phase (Figure 3a). In AISI 304 N stainless steel the  $\sigma$  phase is formed by transformation of the  $\delta$  ferrite to the  $\sigma$  phase and secondary austenite due to unsuitable working conditions (Figure 3b). The dendrite  $\sigma$  phase is an unstable morphology and can lead to embrittlement of the stainless steels. Furthermore, dendrite like  $\sigma$  morphology was observed surrounding the  $\delta$  ferrite particles, which meant that the  $\delta \rightarrow \sigma$  phase transformation occurred partially.

A lacy structure of the  $\sigma$  phase in as-rolled AISI 316 stainless steel is shown in Figure 3c where the  $\sigma$  phase precipitates with a fixed crystallographic direction because of the rolling function.

Figure 3d shows the as-rolled microstructure of the  $\sigma$  phase with a 50% rolling ratio in AISI 304 stainless steel, and the  $\sigma$  phase exhibits dispersed globular morphologies. This globular structure is a stable morphology.

The subsequent rolling process can be used to refine the  $\sigma$  phase particles from an unstable dendrite into stable globular morphologies. Hence, the embrittlement of the  $\sigma$  phase is decreased in the stainless steels by the subsequent rolling process, [6, 14].

## 2.2. Precipitation sites of sigma phase

The precipitation sites of  $\sigma$  phase consist of  $\delta/\gamma$  interface boundary, triple point, grain corner and cellular shape which are shown in Figure 4.

### 2.2.1. $\delta/\gamma$ grain boundary precipitation

The  $\sigma$  phase easily precipitates at the  $\delta/\gamma$  phase boundary, which is a region with high concentration of chromium (Figure 4a).

The initial precipitation sites are  $\delta/\gamma$  interphase boundary because it has higher boundary energy and many defects are concentrated here.

Therefore, the precipitation of  $\sigma$  phase takes place preferentially at  $\delta/\gamma$  boundary, and then precipitates toward interior of  $\delta$  ferrite grain. The other precipitation sites were concentrated at  $\delta$  ferrite because  $\sigma$  phase preferred to precipitate at a higher Cr content region.

When the  $\sigma$  phase nucleates at the  $\delta/\gamma$  interphase boundary, some defects disappear, which releases the free energy of the system. Consequently, the activation energy barrier to form a coherent interface is reduced. Furthermore, the formation of the  $\sigma$  phase is strongly affected by the coherency and interfacial energy of the  $\delta/\gamma$  interface.

This case is typical for austenitic stainless steels.

### 2.2.2. Triple point precipitation

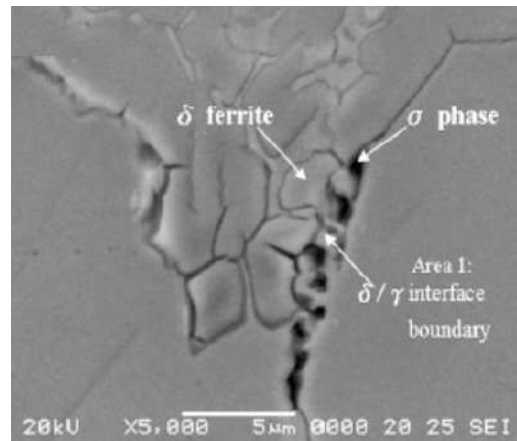
The  $\sigma$  phase also precipitates at the triple point of the  $\delta$  ferrite boundary and this precipitation type, called the “triple point  $\sigma$  phase” (Figure 4b).

The precipitation at triple point means the  $\sigma$  phase precipitated surrounding  $\delta$  ferrite, and according to some authors,  $\sigma$  phase precipitates first on triple points and then on grain faces.

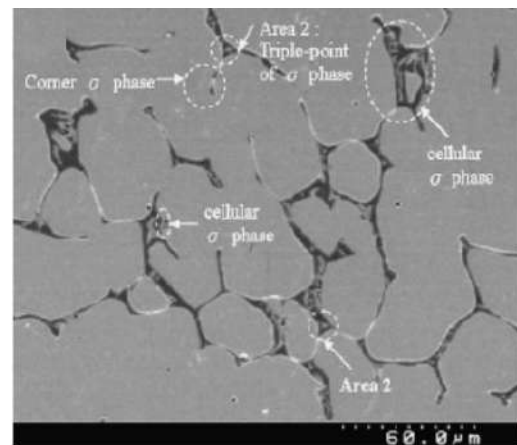
After long- term aging at high temperature, it also forms on the coherent twin boundaries and intragranular inclusions.

### 2.2.3. Corner Precipitation

The precipitation at grain corner means that  $\sigma$  phase is strongly concentrated and formed at the corner of  $\delta$  ferrite particles (Figure 4b) because the  $\delta$  ferrite has a high Cr content phase, and  $\sigma$  phase prefers to nucleate and precipitate at that point. When the  $\sigma$  phase precipitates at the corner of  $\delta$  ferrite, it consumes the Cr from the  $\delta$  ferrite particles.



a)



b)

Figure 4. Precipitation of  $\sigma$  phase at: a)  $\delta/\gamma$  interface boundary and b) triple point, grain corner and cellular [15].

### 2.2.4. Cellular Precipitation

The cellular shape precipitation presents the eutectoid decomposition of  $\delta$  ferrite into  $\sigma$  and secondary austenite ( $\gamma_2$ ) phases ( $\delta \rightarrow \sigma + \gamma_2$ ), Figure 4b. By cellular precipitation  $\sigma$  phase and secondary austenite ( $\sigma + \gamma_2$ ) precipitate as laminar precipitation in the  $\delta$  ferrite particles. When the eutectoid decomposition of  $\delta \rightarrow \sigma + \gamma_2$  is finished, the  $\sigma$  phase consumes the Cr, Mo and Si from the  $\delta$  ferrite particles [6, 15].

Figure 5 summarises the precipitation sequence of the  $\sigma$  phase in various sites of the austenitic stainless steels in a schematic form.

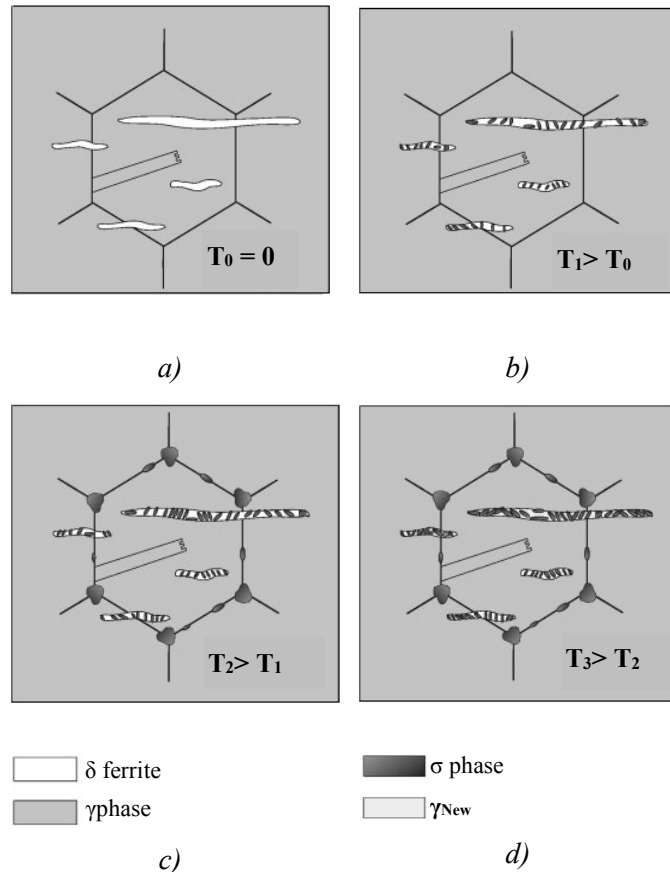


Figure 5. Schematic representation of the  $\sigma$  phase precipitation in AISI 316L austenitic stainless [10].

The precipitation mechanism of the  $\sigma$  phase in the as-rolled plate of austenitic steel 17Cr-12Ni-2.4Mo (AISI 316L) was considered at different aging temperatures (Figures 5a-d).

Without heating i.e. in the case of initial state ( $T_0$ ) the  $\delta$  ferrite with a lacy structure precipitates at the  $\delta/\gamma$  interphase boundary and  $\gamma$  phase (Figure 5a).

When the aging temperature is increased to  $T_1$ , the  $\sigma$  and  $\gamma_2$  phases precipitate in  $\delta$  ferrite particles (Figure 5b), and the cellular  $\sigma + \gamma_2$  also forms in  $\delta$  ferrite particles when the aging temperature increases to  $T_2$  (Figure 5c). In this case the  $\sigma$  phase precipitates at the triple points and the  $\delta/\gamma$  interphase boundaries.

When the aging temperature is  $T_3$  (Figure 5d), the precipitation of the laminar  $\sigma + \gamma_2$  is more expressed than at the other aging (annealing) temperatures, [6, 10].

## 3. EFFECT OF THE SIGMA PHASE ON THE PROPERTIES OF AUSTENITIC STAINLESS STEELS

As previously mentioned that the  $\sigma$  phase is hard, brittle and nonmagnetic at room temperature, therefore it has a negative effect on the mechanical properties. Accordingly, this phase increases the hardness and decreases the toughness, as well as the elongation of the austenitic steel and also changes the fracture type from transgranular to intergranular as the quantity of  $\sigma$  phase increases, [11].

### 3.1. Formation of brittle region

The brittle  $\sigma$  phase generally occurs during the welding of austenitic stainless steels at a temperature interval of 650°C to 900°C and its influence on the material embrittlement appearance depends on its quantity and distribution.

Since, the precipitation of the  $\sigma$  phase decreases the toughness and elongation, the welding energy and cooling rate must be controlled during welding in order to prevent its precipitation as well as the grain growth.

An embrittlement region of  $\sigma$  phase can be shown in Schaeffler diagram of Figure 6.

In Figure 6 it can be seen dark gray region that is prone to occurrence of the  $\sigma$  phase. This is a region with the mixed austenitic-ferritic microstructure (A+F). On the other hand, the single austenite phase region (A) shows a small embrittlement range of the  $\sigma$  phase. Therefore, the possibility of the  $\sigma$  phase is lower in austenitic stainless steels. However, as can be seen in Figure 6, increasing the Cr content i.e.  $Cr_{eq}$  can intensify the precipitation of the  $\sigma$  phase, [6].

Since one of the most affected mechanical properties of steels by formation of the  $\sigma$  phase is impact energy, thus e.g. in Fe-25Cr-20Ni austenitic stainless steel by increasing the time of exposure at formation temperature range of  $\sigma$  phase (760°C – 870°C), toughness value decreases by 85%. Therefore, a relatively small quantity of the  $\sigma$  phase, when it is nearly continuous at a grain boundary, can lead to very early failure of high-temperature parts, [16].

### 3.2. Hot cracking

Hot cracks occur during welding, casting or hot processing at temperatures near the melting point of the material. In austenitic stainless steel hot cracking is amplified by segregation of silicon, phosphorus, sulphur and formation of low melting eutectics in interdendritic regions.

As the content of  $\delta$  ferrite in the weld metal increases, the tendency to form hot cracks increases, so in order to prevent it is specified limit of  $\delta$  ferrite content from 3% to 12% in welded joints. In fact, the ferrite must be maintained to a minimum content to avoid brittleness in service and also avoid generation of cracks during weldments heating, [17, 18].

During the phase transformation  $\delta \rightarrow \sigma$ , it is determined that in austenitic stainless steel weld metals the hot cracking extends along the  $\gamma/\sigma$  interface boundaries. Therefore,  $\gamma/\sigma$  interface boundaries are an initial fracture position of low elongation, whereat crack is a beneficial site and acts as a nucleated point of the  $\sigma$  phase [19].

It was also found that  $\sigma$  phase and hot cracking appeared along the diffusion zone of AISI 316L stainless steel welded joint as shown in Figure 7, [20].

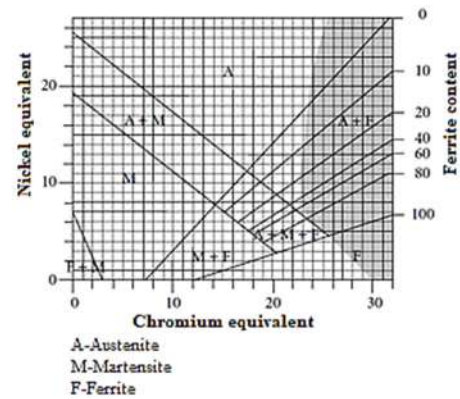


Figure 6. Schaeffler diagram showing the embrittlement region of the  $\sigma$  phase [6].

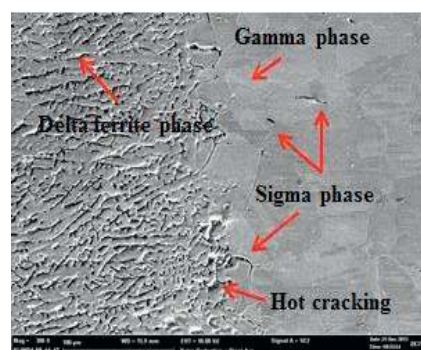


Figure 7. Sigma phase distribution and appearance of hot cracking in 316 stainless steel welded joint, achieved by FESEM – EDX, mag. 300x[20].

### 3.3. Formation of depleted Cr region and reduction of corrosion resistance

The precipitation of the  $\sigma$  phase reduces pitting and intergranular corrosion resistance.

Pitting corrosion always happens at low Cr content and mainly the austenitic boundary is a preferential site for pitting corrosion because the austenite has a low Cr content. However, the depleted Cr zone disappears gradually as a function of Cr diffusion, which issues from the austenite but not the  $\delta$  ferrite. Thereby,  $\sigma$  phase always forms at the  $\delta/\gamma$  interface boundaries and causes the formation of a depleted zone.  $\gamma$  (austenite) and  $\sigma$  phase cause the galvanic effect, and the  $\gamma$  is corroded preferentially, leading to a decrease corrosion resistance.

Generally, the difference in Cr content between the  $\sigma$  phase and secondary austenite (chromium depleted zone) increases with annealing (aging) time due to the continuous diffusion of chromium into  $\sigma$  phase. As the resistance of austenitic stainless steels to pitting corrosion is especially controlled by the content of chromium, molybdenum and nitrogen, the potential resistance of steels to pitting corrosion can be estimated using the so-called PREN, calculated by formula:

$$\text{PREN} = \% \text{Cr} + 3.3\% \text{Mo} + 16\% \text{N} \quad \dots(1)$$

Therefore, the higher value of PREN indicates the more resistant steel against pitting corrosion, [6, 21].

The fine  $\sigma$  phase has a more obvious effect on intergranular corrosion resistance unlike the coarser  $\sigma$  phase, because the fine  $\sigma$  phase forms a network structure at the interface boundary. The coarse particles precipitate independently at the interface, so coarse structure of  $\sigma$  phase has no influence on intergranular corrosion resistance, [6].

## 4. CONCLUSION

It can be concluded that in the austenitic stainless steel, formation of  $\sigma$  phase at elevated temperatures (from 600°C to 900°C) is mainly occurred at grain boundaries ( $\delta/\gamma$ ) and in the  $\delta$  ferrite islands (high Cr concentrated region).  $\sigma$  phase usually precipitates in dendrite of the  $\delta$  ferrite and this is the typical precipitation unstable morphology of the  $\sigma$  phase that can lead to embrittlement of the stainless steels, unlike the globular stable morphology. Also, the presence of  $\delta$  ferrite intensifies  $\sigma$  phase precipitation i.e. reduces the incubation period for  $\sigma$  phase formation. In general, all of the elements that stabilize ferrite rapidly leads to the formation of the  $\sigma$  phase (Cr, Si, Ti, Mo, etc.), while carbon (C) and nitrogen (N) as the austenite stabilizing elements retard  $\sigma$  phase formation. So, it is difficult to prevent the precipitation of the  $\sigma$  phase when the Cr content is above a certain level (above 20 wt.%) in austenitic stainless steels.

The precipitation of hard, brittle and nonmagnetic  $\sigma$  phase at elevated temperatures not only results in harmful influence on the mechanical properties of the material, but also reduces its corrosion resistance by removing chromium and molybdenum from the austenitic matrix. In the presence of  $\sigma$  phase, the tendency to form hot cracks during welding or heat treatment is increased, thereby reducing the toughness and elongation, as well as the formation of the chromium depletion zone and thus reducing the corrosion resistance. Therefore, a relatively small amount of the  $\sigma$  phase can lead to early failure of high-temperature parts.

## 5. REFERENCES

- [1] Padilha, A. F., Rios, P. R.: *Decomposition of Austenite in Austenitic Stainless Steels*, ISIJ International, vol. 42, no. 4, pp. 325–337, 2002.
- [2] <http://www.stainless-steel-world.net/basicfacts/stainless-steel-and-its-families.html>[05.02.2020.]



- [3] Gigović-Gekić, A., Oruč, M., Muhamedagić, S.: *EFFECT OF DELTA FERRITE CONTENT ON THE TENSILE PROPERTIES IN NITRONIC 60 STEEL AT ROOM TEMPERATURE AND 750 °C*, *Materiali in Tehnologije*, volume 46, pp. 519-523, 2012.
- [4] Plaut, R. L., Herrera, C., Escriba, D. M., Rios, P. R., Padilha, A. F.: *A Short Review on Wrought Austenitic Stainless Steels at High Temperatures: Processing, Microstructure, Properties and Performance*, *Materials Research*, vol. 10, no. 4, 453-460, 2007.
- [5] Parrens, C., Lacaze, J., Malard, B., Dupain, J. L., Poquillon, D.: *Isothermal and Cyclic Aging of 310S Austenitic Stainless Steel*, *Metallurgical and Materials Transactions A*, Springer Verlag/ASM International, 48 (6), pp. 2834-2843, 2017.
- [6] Hsieh, C.C., Wu, W.: *Overview of Intermetallic Sigma Phase Precipitation in Stainless Steels*, International Scholarly Research Network, ISRN Metallurgy, pp. 1-16, vol. 2012.
- [7] Kuboň, Z.; Stejskalová, Š., Kander, L.: *Effect of Sigma Phase on Fracture Behaviour of Steels and Weld Joints of Components in Power Industry Working at Supercritical Conditions*. IntechOpen: *Austenitic Stainless Steels - New Aspects*, 2017.  
<http://dx.doi.org/10.5772/intechopen.71569>
- [8] Weiss, B., Stickler, R.: *Phase instabilities during high-temperature exposure of 316 austenitic stainless steel*, *Metall. Trans.*, 3(4):851-866, 1972.
- [9] Restrepo Garcés, G., Le Coze, J., Garin, J. L., Mannheim, R. L.:  *$\sigma$  phase precipitation in two heat-resistant steels – influence of carbides and microstructure*. *Scripta Materialia*, 50 (5): 651-654, 2004.
- [10] Villanueva, D. M. E., Junior, F. C. P., Plaut, R. L., Padilha, A. F.: *Comparative study on sigma phase precipitation of three types of stainless steels: austenitic, superferritic and duplex*, *Materials Science and Technology*, vol. 22, no. 9, pp. 1098–1104, 2006.
- [11] Llorca-Isern, N., López-Luque, H., López-Jiménez, I., Biezma, M. V.: *Identification of sigma and chi phases in duplex stainless steels*, *Materials Characterization*, vol. 112, pp. 20–29, 2016.
- [12] Yakel, H. L.: *Atom Distribution in  $\sigma$  Phases. I. Fe and Cr Atom Distributions in a Binary  $\sigma$  Phase Equilibrated at 1063, 1013 and 923 K*, *Acta Crystallogr. B* 39, 20–28., 1983.
- [13] Folkhard, E.: *Welding Metallurgy of Stainless Steels*, Springer, New York, NY, USA, 1<sup>st</sup> Edition, 1988.
- [14] Hsieh, C.C., Lin, D.Y. and Wu, W.: “*Precipitation Behavior of  $\sigma$  Phase in 19Cr-9Ni-2Mn and 18Cr-0.75Si Stainless Steels Hot-Rolled at 800 °C with Various Reduction Ratios*”, *Materials Science and Engineering A*, vol. 467, no. 1-2, pp. 181–189, 2007.
- [15] Hsieh, C.C., Lin, D.Y., Chang, T.C.: “*Microstructural Evolution During the  $\delta/\sigma/\gamma$  Phase Transformation of the SUS 309LSi stainless Steel after Aging under Various Nitrogen Atmospheric Ratios*”, *Materials Science and Engineering A*, vol. 475, no. 1-2, pp. 128–135, 2008.
- [16] Bina, M. H.: *Homogenization Heat Treatment to Reduce the Failure of Heat Resistant Steel Castings*. IntechOpen: *Metallurgy – Advances in Materials and Processes*, 2012.  
<http://dx.doi.org/10.5772/50312>
- [17] Sejš, P., Kubiček, R.: *Influence of Heat Input on the Content of Delta Ferrite in the Structure of 304L Stainless Steel GTA Welded Joints*, Volume 19, pp. 8-14, 2012.
- [18] Kožuh, S., Gojić, M., Ivanić, I., Kosec, B.: *Microstructure of welded austenitic stainless steel after annealing at 900 °C*, *Zavarivanje i zavarene konstrukcije*, 58 (2013), 4; pp. 149-156.
- [19] Konosu, S., Mashiba, H., Takeshima, M., Ohtsuka, T.: *Effects of pretest aging on creep crack growth properties of type 308 austenitic stainless steel weld metals*, *Engineering Failure Analysis*, vol. 8, no. 1, pp. 75–85, 2001.
- [20] Moslemi, N., Redzuan, N., Ahmad, N., Hor, T. N.: *Effect of Current on Characteristic for 316 Stainless Steel Welded Joint Including Microstructure and Mechanical Properties*, *Procedia CIRP*, vol. 26, pp. 560 – 564, 2015.
- [21] Khatak, H. S., Raj, B.: *Corrosion of Austenitic Stainless Steels: Mechanism, Mitigation and Monitoring*, 1<sup>st</sup> Edition, pp. 400, 2002.